YMTHE, Volume *30*

Supplemental Information

CircRNA Samd4 induces cardiac repair after myocardial infarction by blocking mitochondria-derived ROS output

Hao Zheng, Senlin Huang, Guoquan Wei, Yili Sun, Chuling Li, Xiaoyun Si, Yijin Chen, Zhenquan Tang, Xinzhong Li, Yanmei Chen, Wangjun Liao, Yulin Liao, and Jianping Bin

Supplemental figures and legends

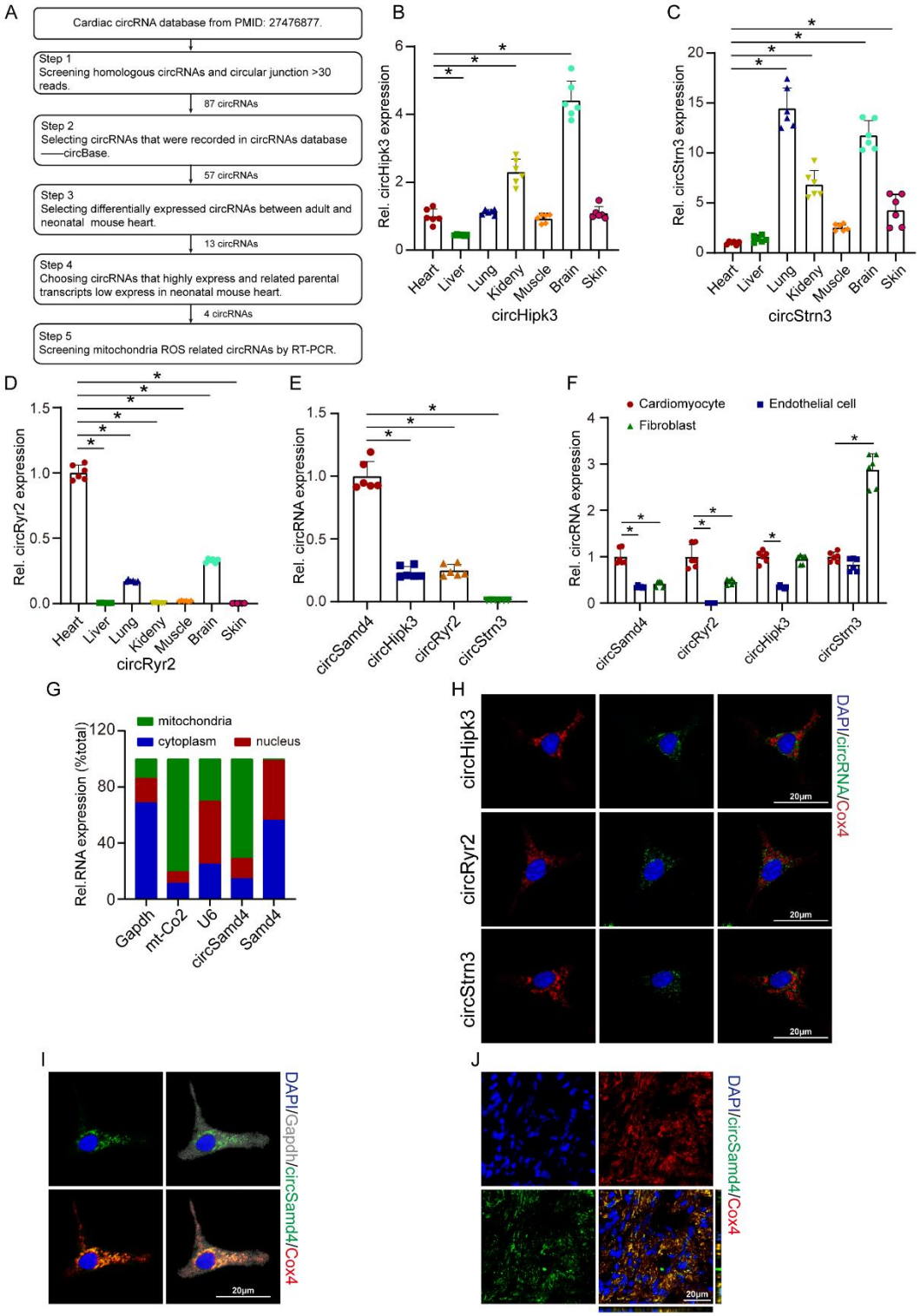

Figure S1. Identification of neonatal CM-enriched circRNAs that are involved in antioxidative response. (A) Illustration of steps for identifying and validating neonatal CM-enriched circRNAs that are involved in antioxidative response. (B-D)

The relative expression levels of indicated circRNAs in multiple types of tissues in neonatal mouse; *P<0.05 vs. heart in each group, n=6; (E) The relative expression levels of indicated circRNAs in myocardium of neonatal mouse; *P<0.05 vs. circSamd4, n=6; (F) The relative expression levels of indicated circRNAs in P1 CM, cardiac endothelial cell and cardiac fibroblast; *P<0.05 vs. CM in each group, n=6; (G) CircSamd4 were detected in nuclei, cytoplasm and mitochondria extract of CM. U6, Gapdh and mt-Co2 was used as the nuclei, cytoplasm and mitochondria marker, respectively. (H) RNA-FISH assay of circHipk3, circRyr2 and circStrn3, coimmunostaining of Cox4 in P1 CMs. (I) RNA-FISH assay of circSamd4, coimmunostaining of Cox4 and Gapdh in P1 CMs. (J) RNA-FISH assay of circSamd4, coimmunostaining of Cox4 in P1 heart tissue.

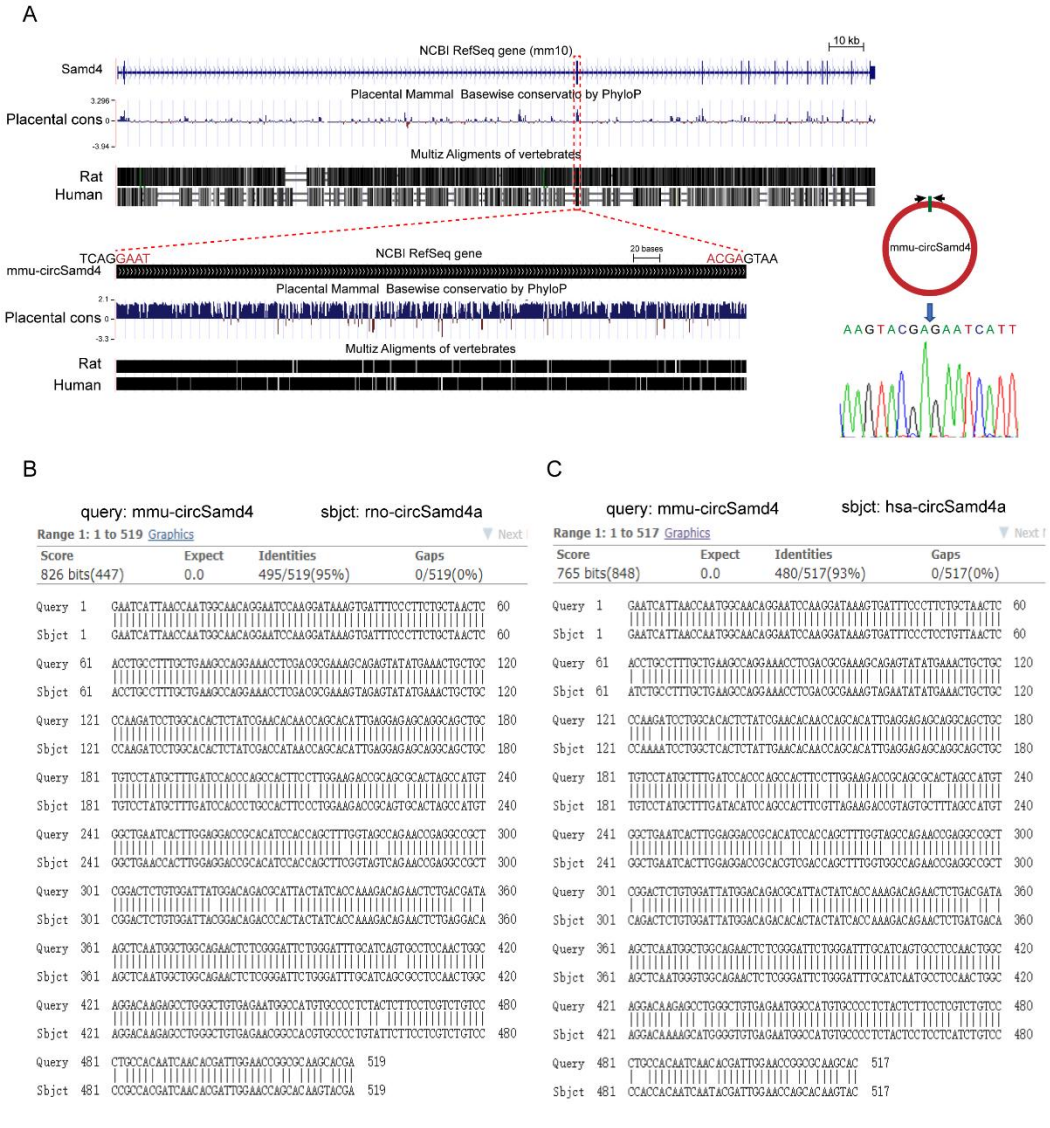

Figure S2. Conservation analysis of circSamd4 sequence. (A) Species conservation analysis showed that the sequence of circSand4a were conserved across humans, mice and rats; the result of Sanger sequencing present in the lower right-hand corner revealed the head-to-tail junction of circSamd4. (B-C) circSamd4 conversation analysis in human, mouse and rat genome was conducted by using Basic Local Alignment Search Tool (BLAST).

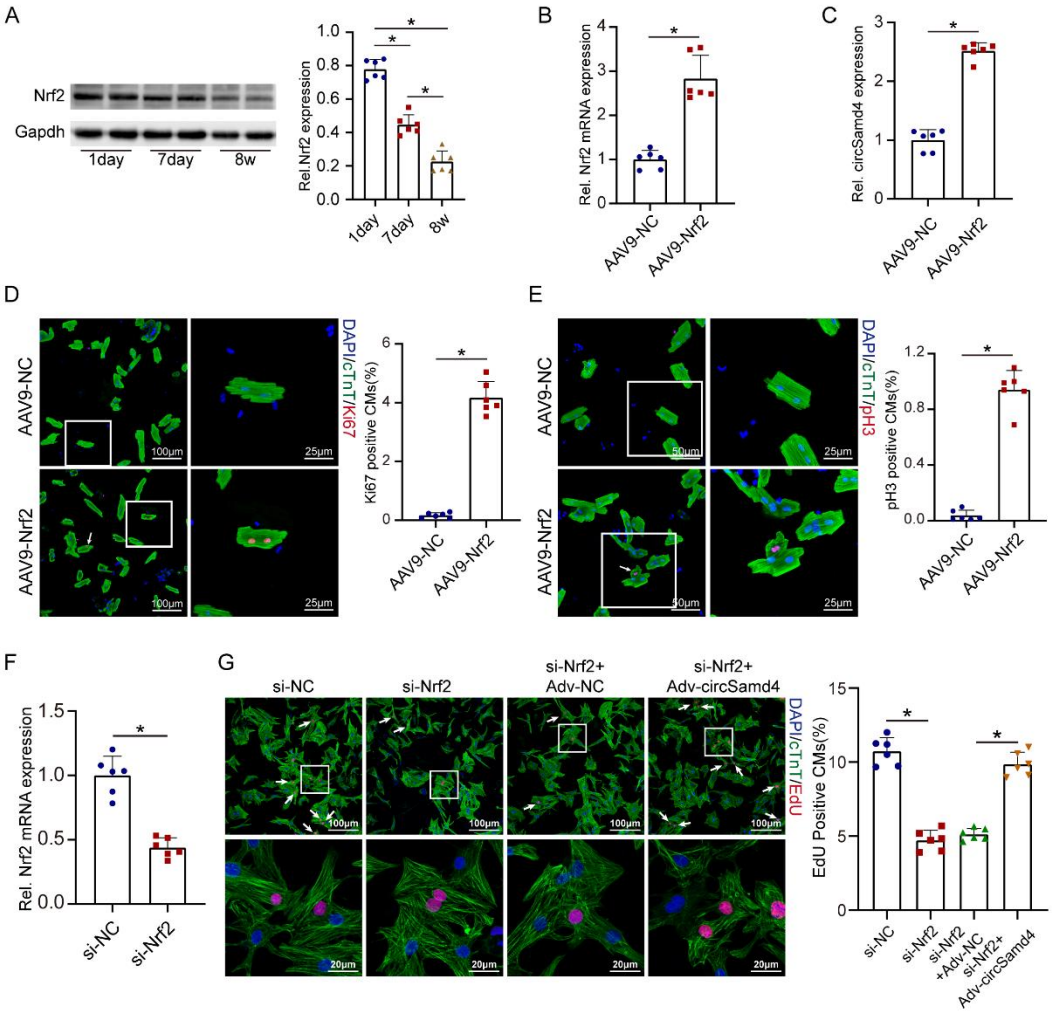

Figure S3. The role of Nrf2 on CM proliferation and cardiac regeneration. (A) Detection of Nrf2 protein expression level in CMs of different developmental stages. **P*<0.05, n=6. (B-C) Detection of Nrf2 and circSamd4 expression level in adult mouse hearts after injection of AAV9-Nrf2 or AAV9-NC. **P*<0.05, n=6. (D) Detection of Ki67+ adult CMs isolated from adult mouse heart after AAV9-Nrf2 and AAV9-NC injection. Ki67+ CMs are indicated by arrows, **P*<0.05, n=6. (E) Detection of pH3+ adult CMs isolated from adult mouse heart after AAV9-Nrf2 and AAV9-NC injection. PH3+ CMs are indicated by arrows, **P*<0.05, n=6. (F) The transfection of Nrf2 siRNA decreased Nrf2 expression in P1 CMs. The Nrf2 mRNA

abundance was detected by qRT-PCR assay. *P<0.05, n=6; (G) Representative images and quantification of EdU+ CMs in P1 CMs after Nrf2 and circSamd4 interference. EdU+ CMs are indicated by arrows, *P<0.05, n=6.

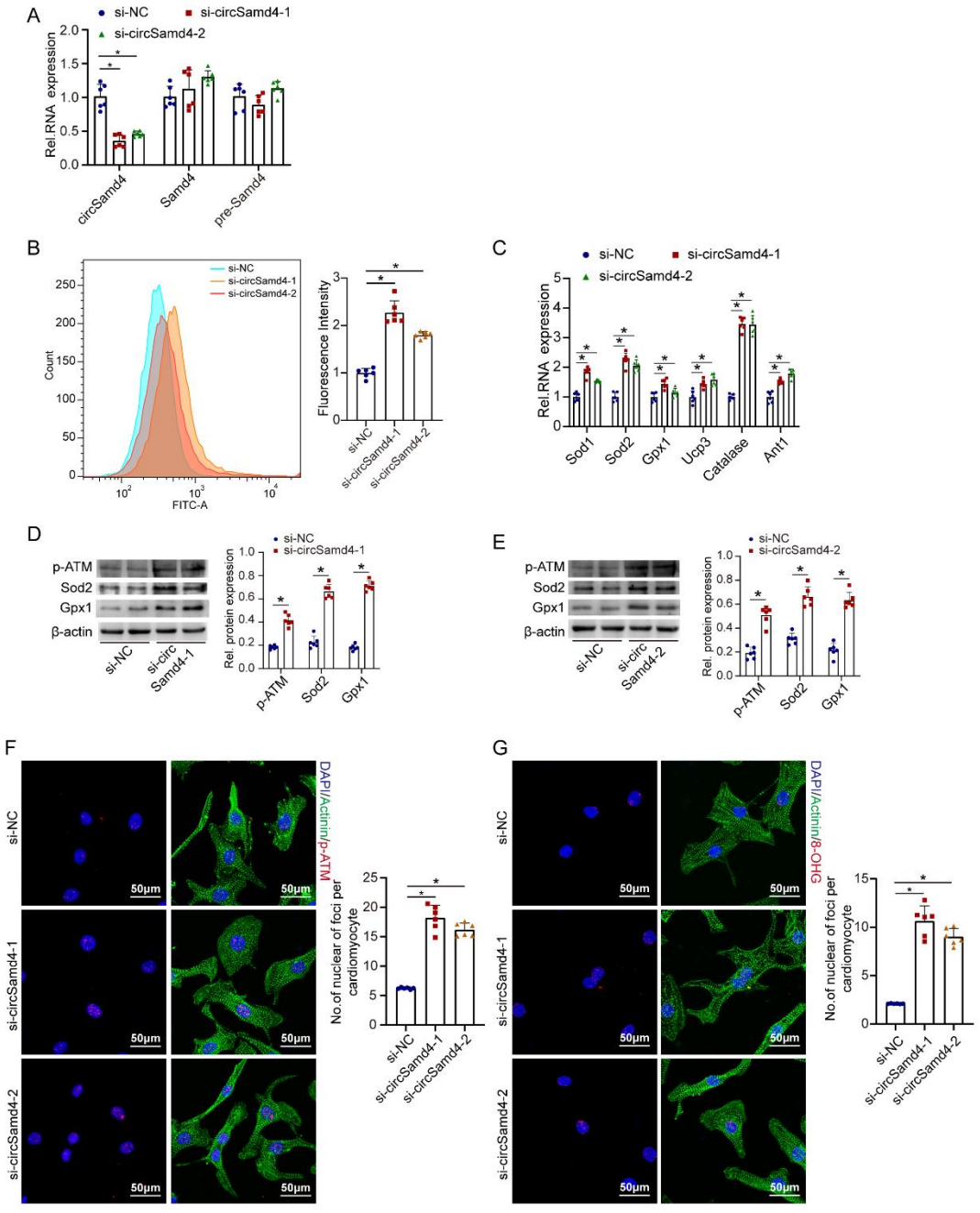

Figure S4. CircSamd4 down-regulation increased intracellular oxidative stress in CMs. (A) Changes in the expression level of circSamd4 after siRNA transfection.

*P<0.05 vs. si-NC, n=6. (B) Quantified cellular oxidative stress by DCFH-DA assay using flow cytometry. *P<0.05 vs. si-NC, n=6. (C) Detection of the expression levels of genes related to oxidative stress in P1 CMs after circSamd4 knockdown or control treatment using qRT–PCR assays. *P<0.05 vs. si-NC, n=6. (D-E) Changes in the expression level of the Sod, Gpx1 and p-ATM protein after circSamd4 knockdown. *P<0.05, n=6. (F) Detection of p-ATM expression in CMs after circSamd4 down-regulation via Immunofluorescence assays. *P<0.05 vs. si-NC, n=6. (G) Detection of 8-OHG expression in CMs after circSamd4 down-regulation via Immunofluorescence assays. *P<0.05 vs. si-NC, n=6.

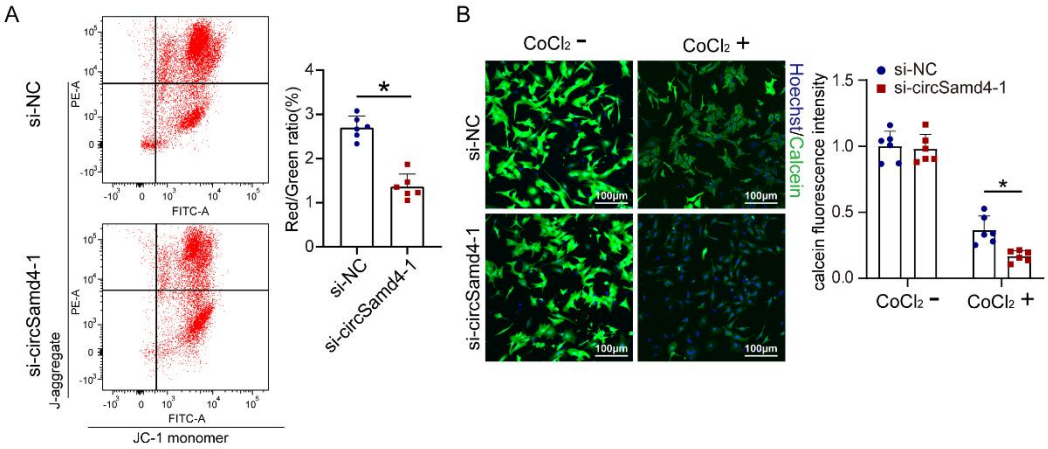

Figure S5. CircSamd4 knockdown promoted MMP opening in CMs *exo vivo*. (A) Detection of the MMP of P1 CMs after circSamd4 interference using flow cytometry assay. *P<0.05, n=6. (B) Detection of the MMP opening status after circSamd4 interference by Calcein-AM/$CoCl_2$ method. *P<0.05, n=6.

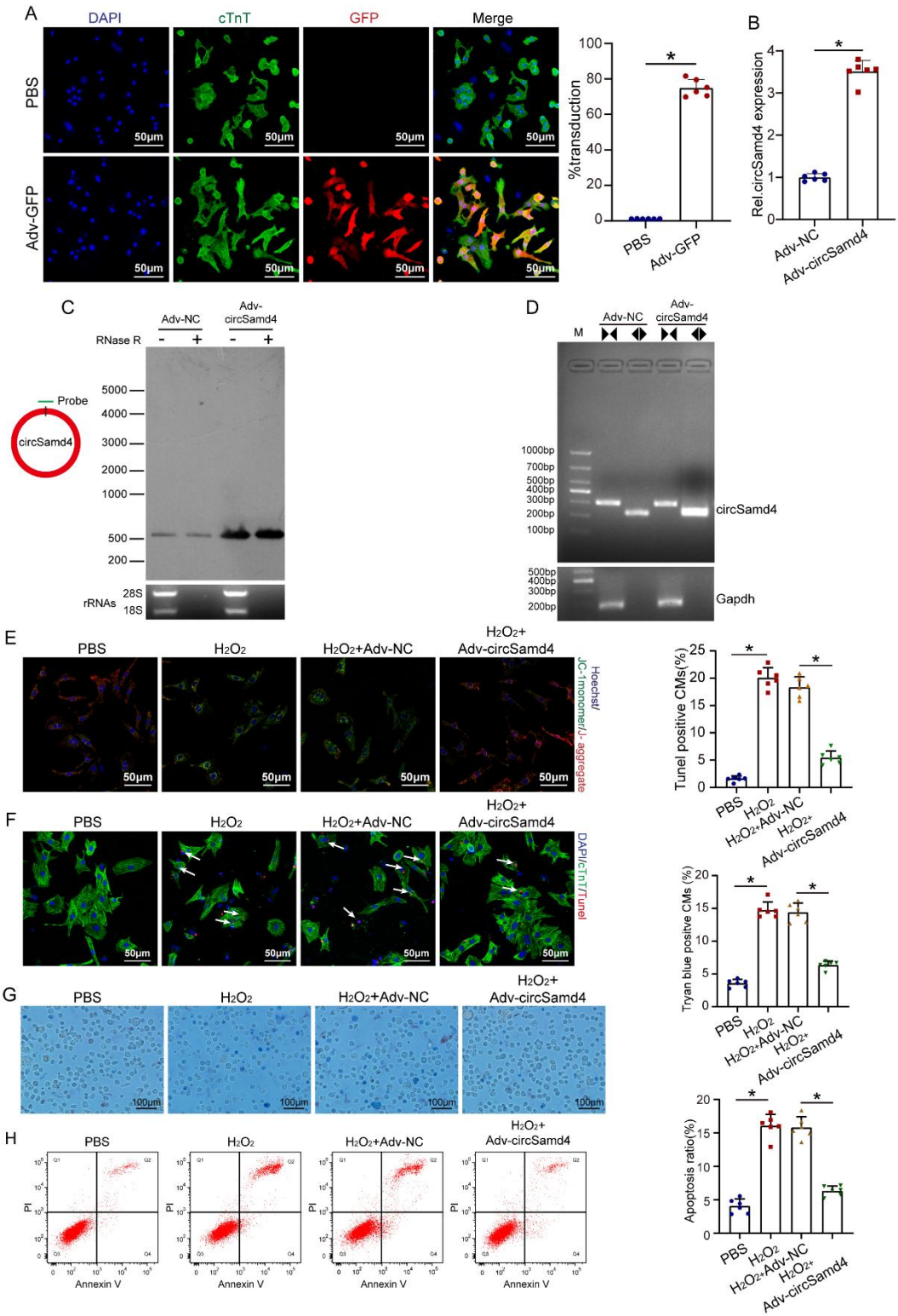

Figure S6. Evaluation of anti-oxidation effect of Adv-circSamd4. (A) GFP/cTnT co-staining in P1 CMs after transduction of Adv-GPF. (B) The transduction of Adv-circSamd4 increased circSamd4 expression in P1 CMs; **P*<0.05, n=6; (C)

Detection of circSamd4 in CMs after Adv-circSamd4 or Adv-NC transfection via Northern blot analysis. The used probe was targeting circSamd4 back-splicing site. (D) Amplification of circSamd4 in cDNA but not genomic DNA using divergent primers; gDNA, genomic DNA. (E) Assessing the MMP of P1 CMs using immunofluorescence assay. P1 CMs were transduced with Adv for 24 h, and then incubated with H_2O_2 (20 μM) for 8 hours. JC-1 monomer: green; J-aggregate: red. (F) Assessing the ratio of apoptotic CMs using TUNEL staining. P1 CMs were transduced with Adv for 24 h, and then incubated with H_2O_2 (20 μM) for 8 hours. TUNEL+ CMs are indicated by arrows, *P<0.05, n=6. (G) Assessing the ratio of death CMs using Trypan Blue Exclusion. P1 CMs were transduced with Adv for 24 h, and then incubated with H_2O_2 (20 μM) for 8 hours. Blue stained, dead CMs. *P<0.05, n=6. (H) Assessing the ratio of apoptotic CMs using Annexin V-FITC/PI fluorescent staining. P1 CMs were transduced with Adv for 24 h, and then incubated with H_2O_2 (20 μM) for 8 hours. *P<0.05, n=6.

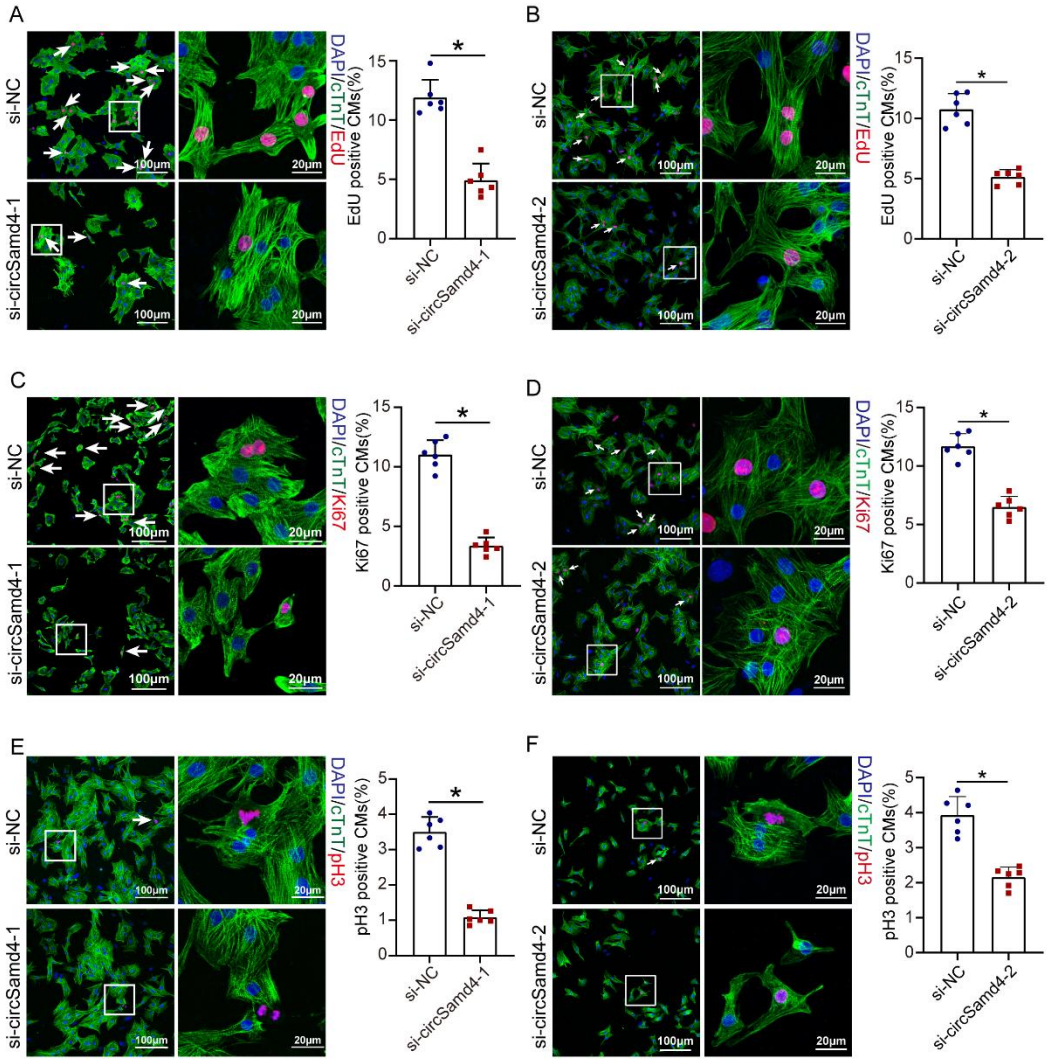

Figure S7. CircSamd4 knockdown repressed neonatal CM proliferative. (A-B) Representative images and quantification of EdU+ CMs in P1 CMs after circSamd4 interference. EdU+ CMs are indicated by arrows, **P*<0.05 vs. si-NC, n=6. (C-D) Representative images and quantification of Ki67+ CMs in P1 CMs after circSamd4 interference. Ki67+ CMs are indicated by arrows, **P*<0.05 vs. si-NC, n=6. (E-F) Representative images and quantification of pH3+ CMs in P1 CMs after circSamd4 interference. pH3+ CMs are indicated by arrows, **P*<0.05 vs. si-NC, n=6.

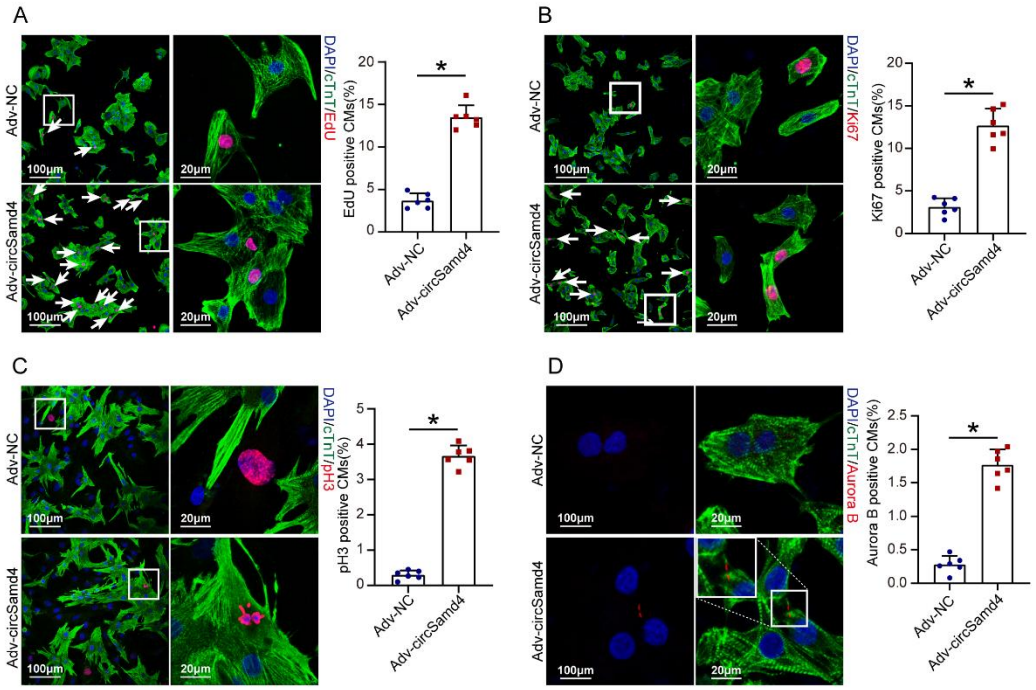

Figure S8. CircSamd4 overexpression promoted P7 CM proliferation *in vitro*. (A) Representative images and quantification of EdU+ CMs after circSamd4 overexpression; **P*<0.05, n=6. (B) Representative images and quantification of Ki67+ CMs after circSamd4 overexpression; **P*<0.05, n=6. (C) Representative images and quantification of pH3+ CMs after circSamd4 overexpression; **P*<0.05, n=6. (D) Representative images and quantification of Aurora B+ CMs after circSamd4 overexpression; *P<0.05, n=6.

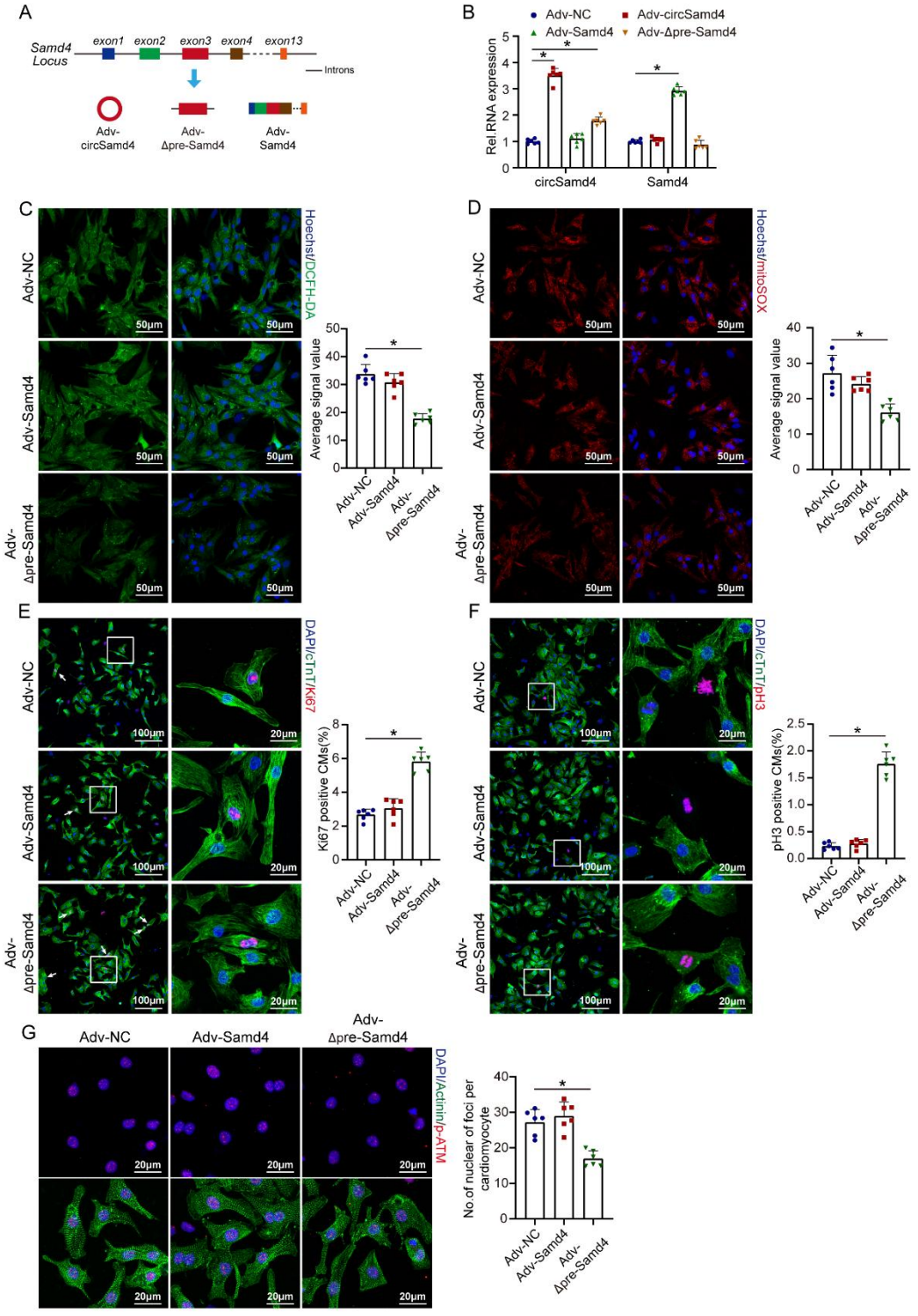

Figure S9. The effect of Samd4 mRNA or Samd4 pre-mRNA overexpression on CM proliferation. (A) The schematics showed that sequence of Adv vector encoding for circSamd4, Samd4 mRNA and Samd4 pre-mRNA fragment. Δpre-Samd4: Samd4 pre-mRNA fragment containing exon3 and its flanking sequences (2.5kb). (B)

Detection of circSamd4 and Samd4 mRNA expression level after different Adv vector transfection in P1 CMs; *P<0.05, n=6. (C-D) Detection of cytosolic (C) and mitochondrial (D) ROS in CMs by confocal microscopy; *P<0.05, n=6. (E) Evaluation of CM proliferative activity by Ki67 immunostaining after Adv vector transfection. Ki67+ CMs are indicated by arrows, *P<0.05, n=6. (F) Evaluation of CM proliferative activity by pH3 immunostaining after Adv vector transfection. pH3+ CMs are indicated by arrows, *P<0.05, n=6. (G) Transfection of vector for Samd4 pre-mRNA fragment reduced DNA damage induced by H_2O_2. CMs were transduced with Adv for 24 h and then incubated with H_2O_2 (20 μM) for 8 hours. *P<0.05, n=6.

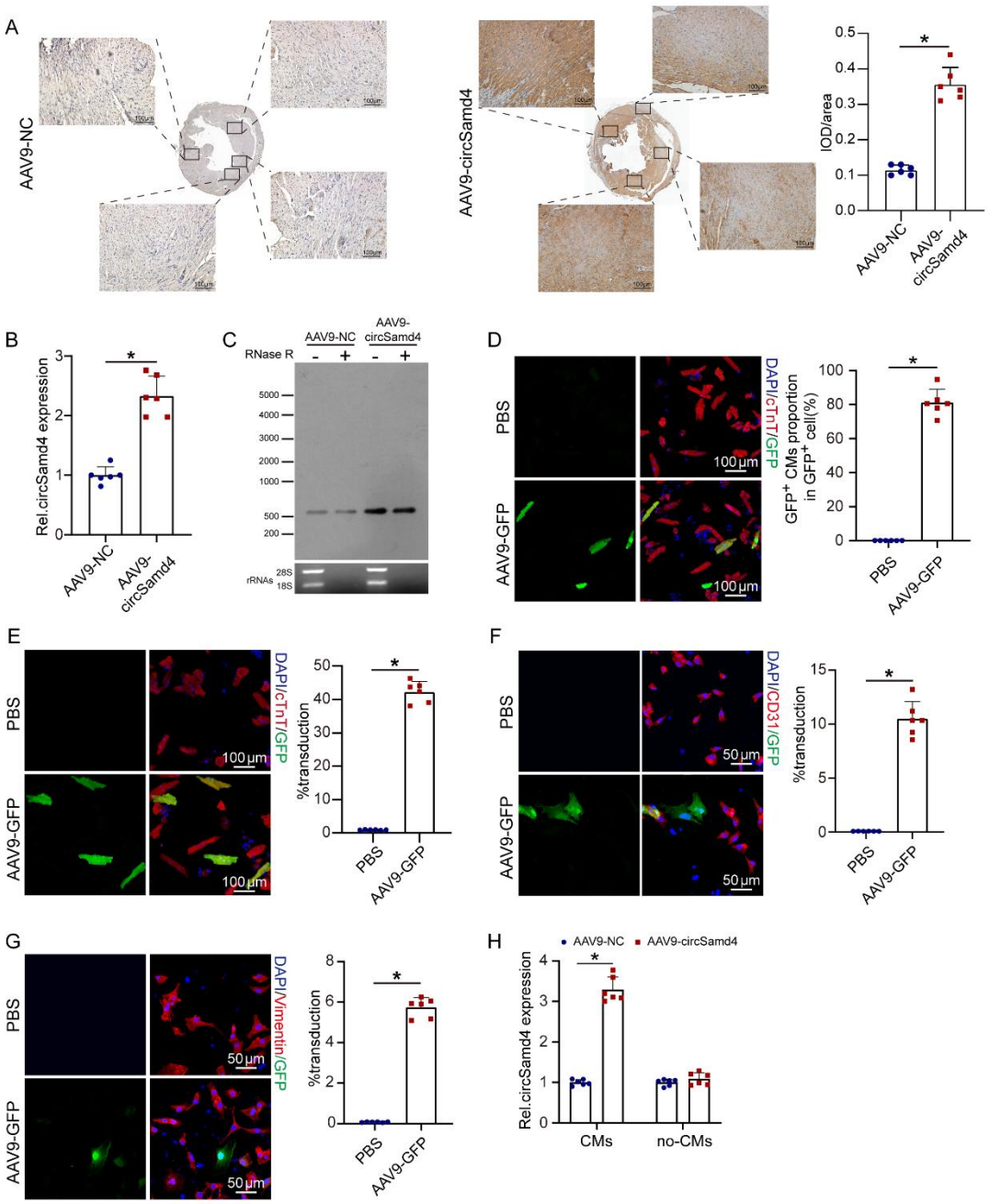

Figure S10. Evaluation of transduction efficiency and specificity for AAV9-circSamd4. (A-B) The expression of circSamd4 was increased in adult mouse hearts 14 days after injection of AAV9-circSamd4, compared to AAV9-NC. *P<0.05. (A): ISH assays of circSamd4 in heart sections was conducted on 4 sections per sample and images from 4 different randomly selected area were acquired, n=6. (B): PCR assays, n=6. (C) Detection of circSamd4 in myocardium tissue after

AAV9-circSamd4 or AAV9-NC infection via Northern blot analysis. The used probe was targeting circSamd4 back-splicing site. (D) Representative images and quantification of GFP+ CMs in total GFP+ cells isolated from adult mouse hearts on 14 days after injection of AAV9-GFP or PBS, *P<0.05, n=6. (E) The transduction efficiency in CMs isolated from adult mouse hearts on 14 days after injection of AAV9-GFP or PBS, *P<0.05, n=6. (F) The transduction efficiency in endothelial cells isolated from adult mouse hearts on 14 days after injection of AAV9-GFP or PBS, *P<0.05, n=6. (G) The transduction efficiency in cardiac fibroblasts isolated from adult mouse hearts on 14 days after injection of AAV9-GFP or PBS, *P<0.05, n=6. (H) Detection of circSamd4 expression in adult CMs and non-CMs after AAV9-circSamd4 or AAV9-NC injection. *P<0.05, n=6.

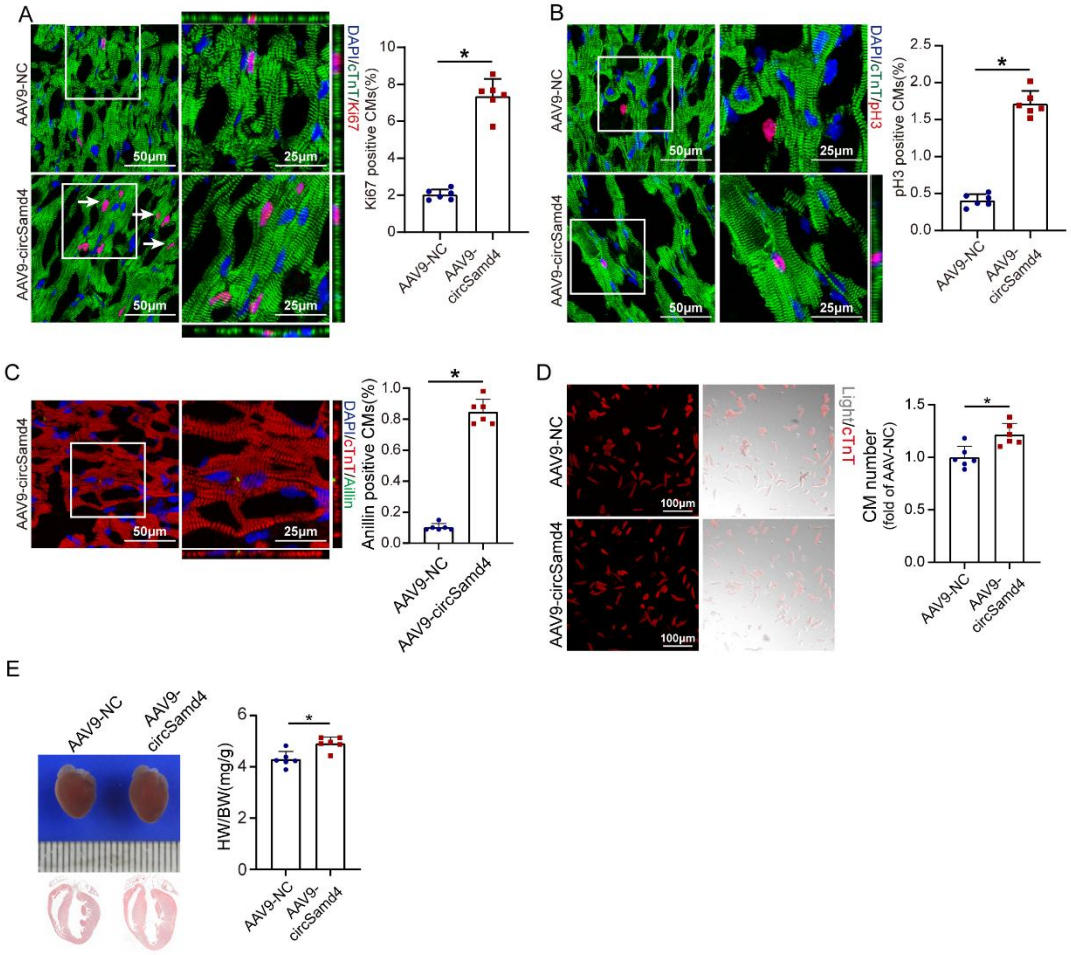

Figure S11. CircSamd4 overexpression promoted CM proliferation in adult mouse hearts *in vivo*. (A) Evaluation of adult CMs proliferation by Ki67 immunostaining 14 days after AAV9-circSamd4 or AAV9-NC injection; **P*<0.05, n=6. (B) Evaluation of adult CMs proliferation by pH3 immunostaining 14 days after AAV9-circSamd4 or AAV9-NC injection; **P*<0.05, n=6. (C) Evaluation of adult CMs proliferation by Anillin immunostaining 14 days after AAV9-circSamd4 or AAV9-NC injection; **P*<0.05, n=6. (D) Comparison of CMs number in adult hearts from AAV9-circSamd4 and AAV9-NC group. Scale bars, 100 μm. **P*<0.05, n=6. (E) Comparison of adult heart weight/body weight ratios between AAV9-circSamd4 and AAV9-NC group. **P*<0.05, n=6.

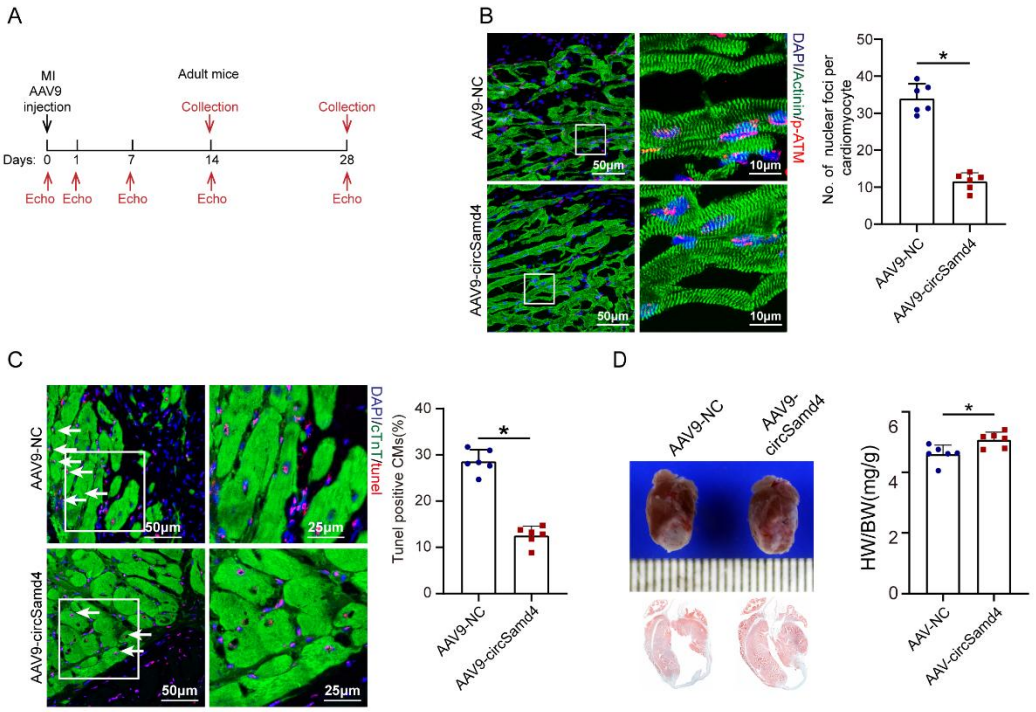

Figure S12. CircSamd4 overexpression alleviated oxidative injury in adult mouse hearts after MI. (A) Schematic of the myocardial infarction (MI) experiments in adult mice. Echo, echocardiography. (B) Detection of DDR in adult CMs 14 days post-MI. *P<0.05, n=6. (C) Detection of apoptotic CMs 14 days post-MI using TUNEL staining. TUNEL+ CMs are indicated by arrows, *P<0.05, n=6. (D) Comparison of heart weight/body weight ratios between AAV9-circSamd4 and AAV9-NC group after MI. *P<0.05, n=6.

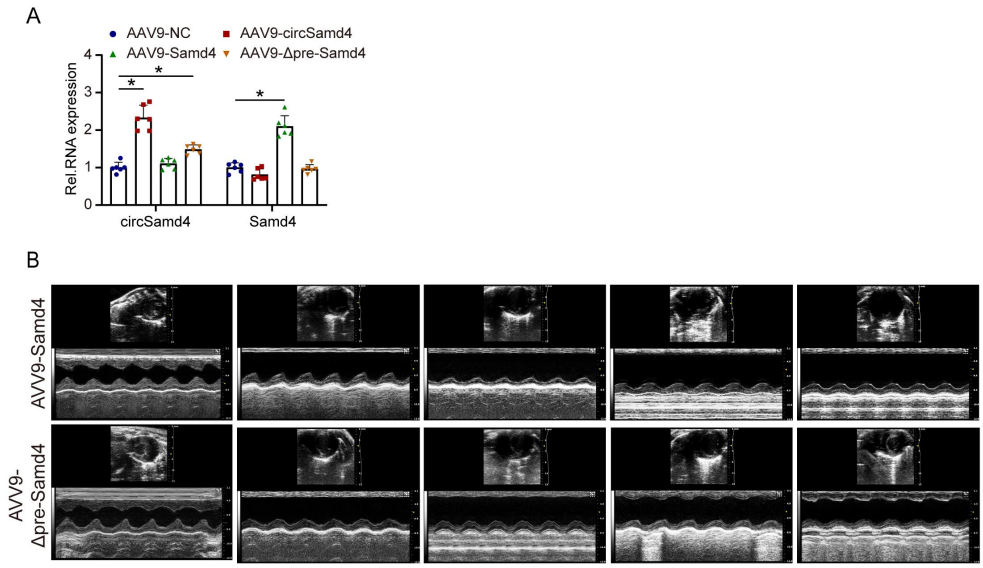

Figure S13. The effect of Samd4 mRNA or Samd4 pre-mRNA overexpression on cardiac function improvement after MI. (A) Detection of circSamd4 and Samd4 mRNA expression level in myocardium tissue after different AAV9 injection; **P*<0.05, n=6. Δpre-Samd4: Samd4 pre-mRNA fragment containing exon3 and its flanking sequences (2.5kb). (B) Evaluation of the left ventricular ejection fraction (LVEF), left ventricular end-systolic dimension (LVESD), left ventricular end-diastolic dimension (LVEDD) and fractional shortening (FS) post-MI after Samd4 mRNA or Samd4 pre-mRNA fragment overexpression. The echocardiography analysis was performed on Days 1, 7, 14 and 28 after surgery. The bar graph was present in Figure 5A.

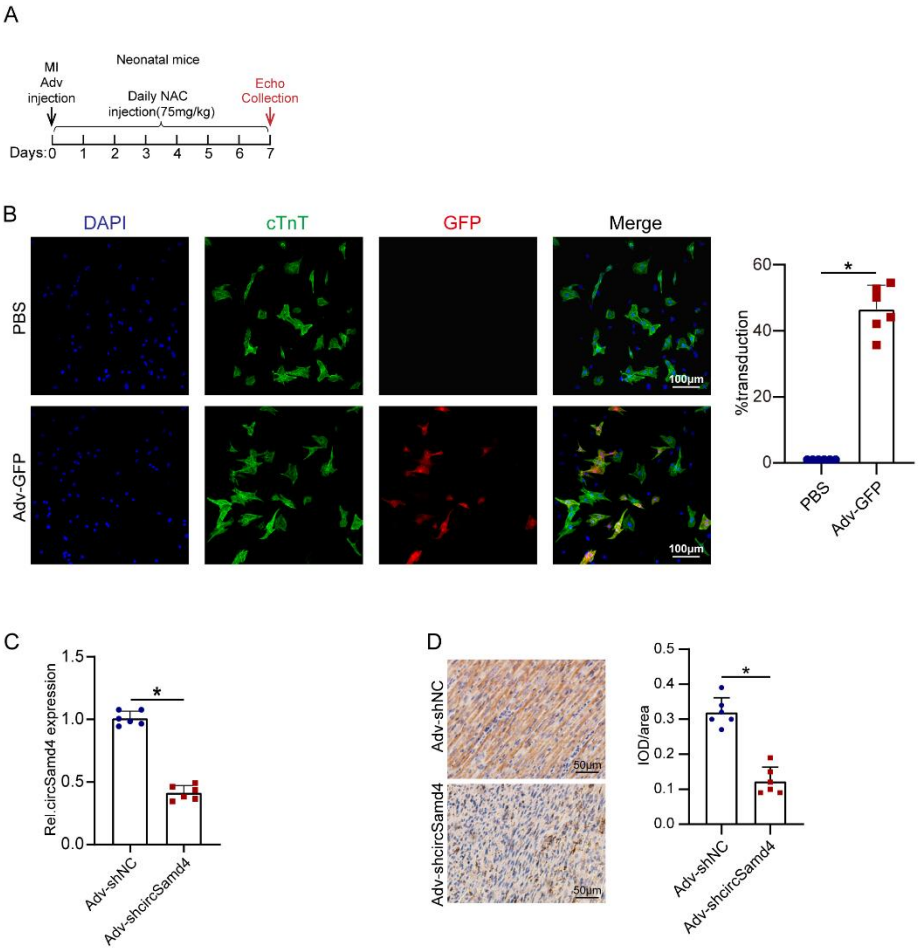

Figure S14. Evaluation of transduction efficiency for Adv-shcircSamd4 in neonatal mouse heart. (A) Schematic of the MI experiments in neonatal mice. NAC, N-Acetyl-L-cysteine; Echo, echocardiography. (B) Representative images and quantification of GFP+ CMs isolated from neonatal mouse hearts on 7 days after injection of Adv-GFP or PBS. **P*<0.05, n=6. (C-D) The injection of Adv-shcircSamd4 reduced circSamd4 expression in neonatal mouse hearts, compared to Adv-shNC; **P*<0.05, n= 6; (C): PCR assays, (D): ISH assays.

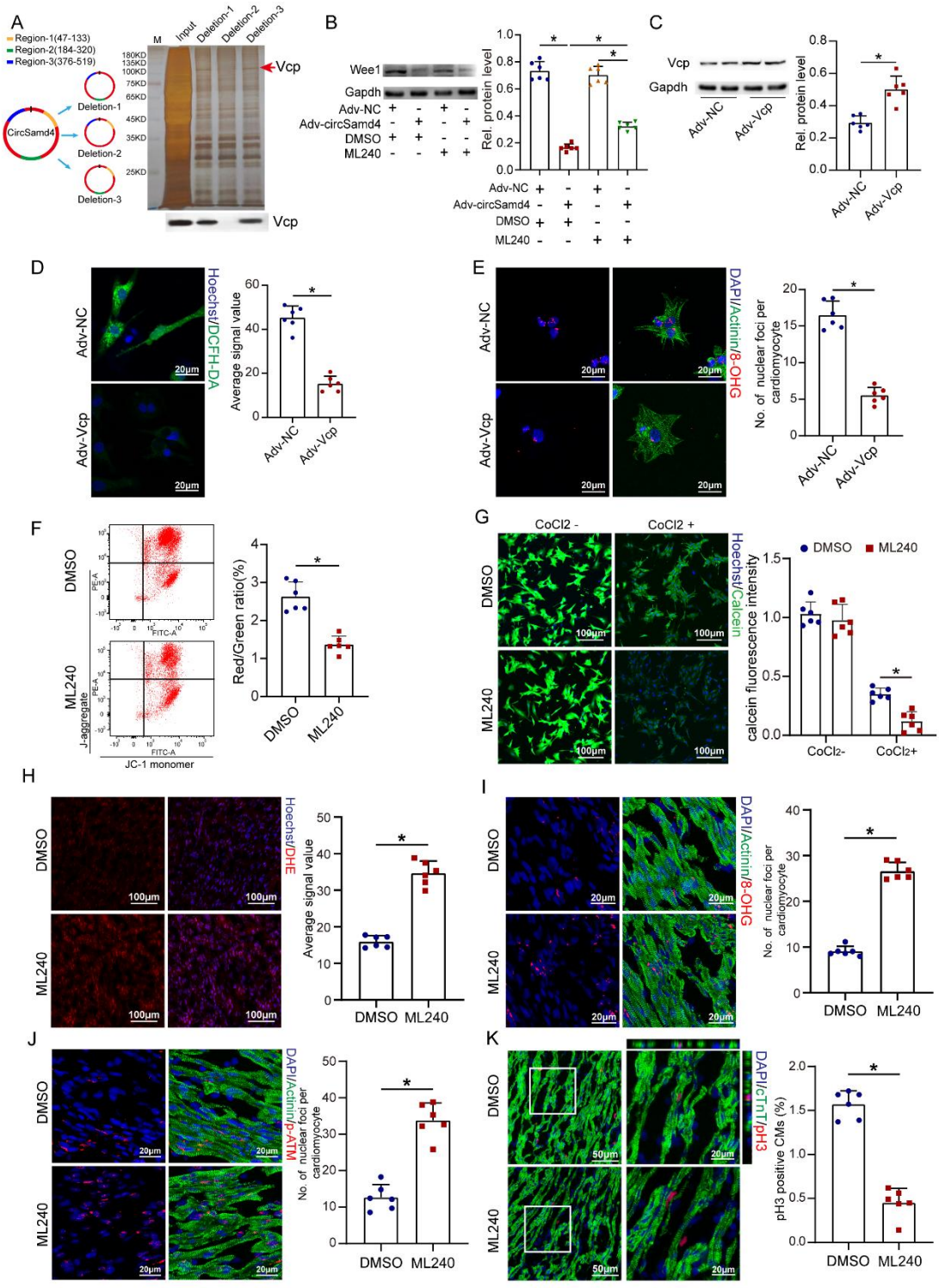

Figure S15. The effect of Vcp overexpression and ML240 treatment on oxidative injury for CMs. (A) The CMs were transfected with circSamd4 mutants. The schematics showed the structure of circSamd4 mutants. The CM lysates were subjected to RNA pull-down and western blot assays. (B) Changes in the expression

level of the Wee1 protein after circSamd4 overexpression and/or 5μM ML-240 treatment; *P<0.05, n=6. (C) Vcp overexpression increased Vcp protein level in P1 CMs; *P<0.05, n=6. (D) Vcp overexpression reduced intracellular ROS level in CMs. P1 CMs were transduced with Adv for 24 h, and then incubated with H_2O_2 (20 μM) for 8 hours. *P<0.05, n=6. (E) Vcp overexpression reduced oxidative DNA damage in CMs. P1 CMs were transduced with Adv for 24 h, and then incubated with H_2O_2 (20 μM) for 8 hours. *P<0.05, n=6. (F) Detection of the MMP of P1 CMs after ML-240 treatment using flow cytometry assay. *P<0.05, n=6. (G) Detection of the MMP opening status of P1 CM after ML-240 treatment by Calcein-AM/$CoCl_2$ method. *P<0.05, n=6. (H) ML240 treatment increased intracellular ROS level in neonatal mouse hearts; *P<0.05, n=6. (I) ML240 treatment induced oxidative DNA damage in neonatal mouse hearts. Neonatal mice were injected with ML240 (1.2mg/kg) subcutaneously every 2 day from day 0-day 7. *P<0.05, n=6. (J) ML240 treatment promoted DDR in neonatal mouse hearts; *P<0.05, n=6. (K) Detection of pH3+ CMs in neonatal mice treated with ML240 or DMSO; *P<0.05, n=6.

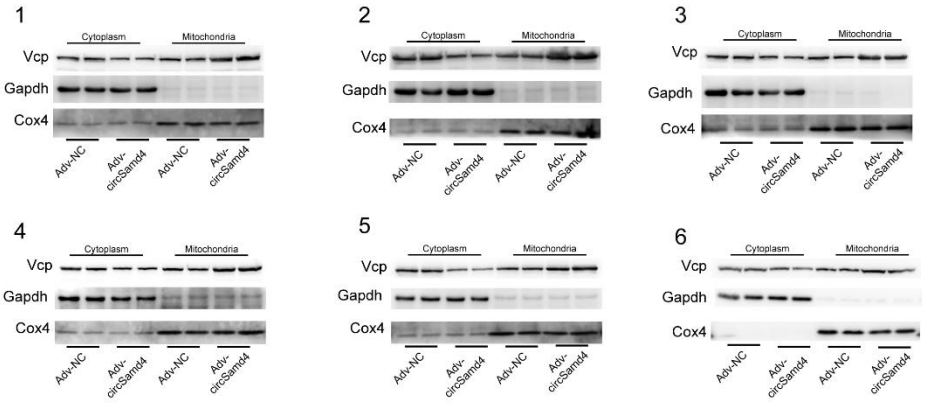

Figure S16. The images used for statistical analysis in the bar graph of Figure 7F.

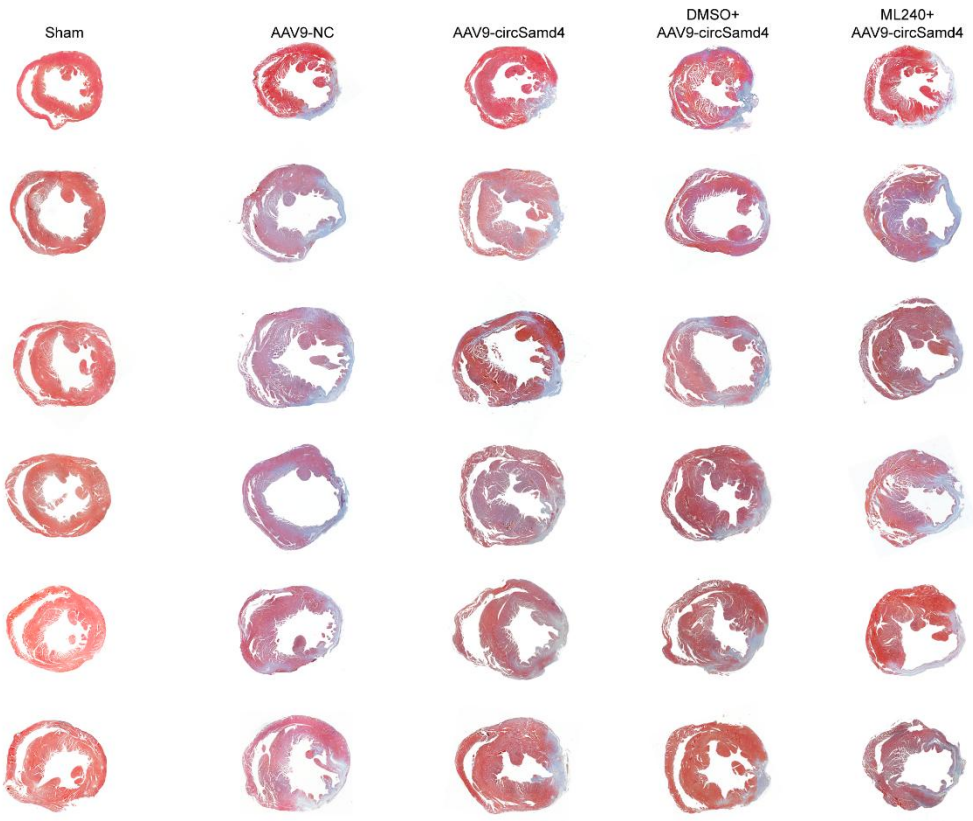

Figure S17. The images used for statistical analysis in the bar graph of Figure 7P.

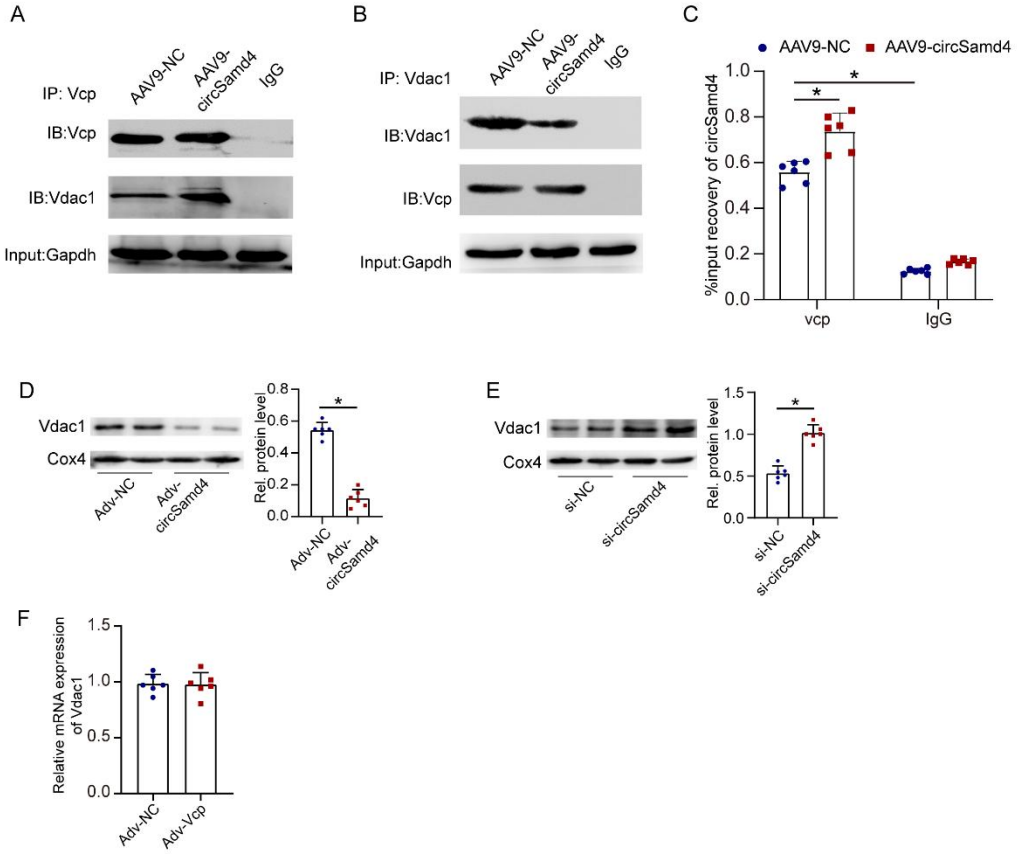

Figure S18. Identification of ternary interaction of circSamd4/Vcp/Vdac1 on peri-infarcted zone. (A) Co-IP assay in border zone of infarcted hearts using antibody to Vcp. (B) Co-IP assay in border zone of infarcted hearts using antibody to Vdac1. (C) RIP assay in border zone of infarcted hearts using antibody to Vcp. **P*<0.05, n=6. (D) Changes in the expression level of the outer mitochondrial membrane protein Vdac1 after circSamd4 overexpression and 20 μM H_2O_2 treatment; **P*<0.05, n=6. Mitochondria were extracted from P1 CMs, and western blotting was then performed to detect the Vdac1. (E) Changes in the expression level of the Vdac1 protein after circSamd4 interference; **P*<0.05, n=6. Mitochondria were extracted from P1 CMs, and western blotting was then performed to detect Vdac1. (F) qRT-PCR assays assessing the expression level of the Vdac1 mRNA in P1 CMs

transduced with Adv-Vcp or Adv-NC. *P<0.05, n=6.

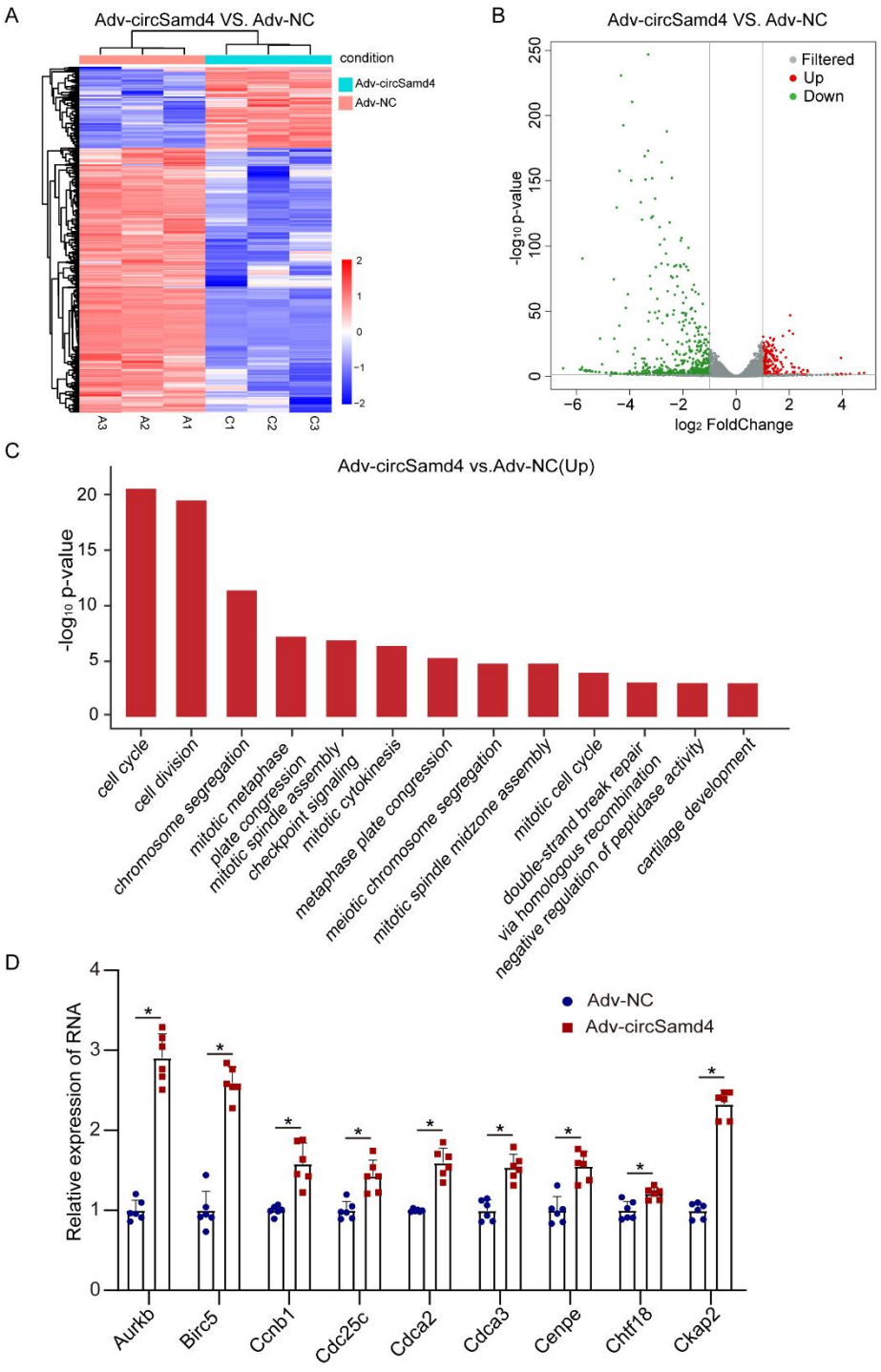

Figure S19. Transcriptional profile of CMs after circSamd4 overexpression. (A) Heatmap highlighted the differentially expressed genes between Adv-circSamd4

transduced CMs and Adv-NC transduced CMs. (B) The volcano plot showed the expression profiling between Adv-circSamd4 transduced CMs and Adv-NC transduced CMs. (C) List of selected significantly enriched GO biological terms for the differentially expressed genes between Adv-circSamd4 transduced CMs and Adv-NC transduced CMs. (D) qRT-PCR assays validated the expression level of several differentially expressed genes involved in cell-cycle progression. *P<0.05, n=6.

Table S1. The primers used for PCR in this study.

Primers/RNA interference name		Sequence (5'-3')
circSamd4	+	TCTACTCTTCCTCGTCTGT
	-	CTCCTCAATGTGCTGGTT
Linear-Samd4 mRNA	+	CGCTACTGTCTGTCATCGTCTC
	-	TCTGCTCGCACTCGTTCC
pre-Samd4	+	CTAAGAACGCCTGGAATCA
	-	CCTGCTCTCCTCAATGTG
Samd4 Site-1	+	TCAATCATCGTTCAAACACCT
	-	CAGCAAGACTTCAAAGATGAACTA
Samd4 Site-2	+	TTACGTTATTGGTGTATCTTTGGT
	-	CATTTCCTGGCAGAAGTACTAC
cricHipk3	+	GGATCGGCCAGTCATGTATC
	-	ACCGCTTGGCTCTACTTTGA
circStrn3	+	GCTGCTGACTTAACTGATG
	-	GTATCTGTGTATCCTACTTCCT
circRyr2	+	CACCGCCTGTACTTCTTG
	-	GGATACCACATAACCACTGAT
Nrf2	+	GTGCTCCTATGCGTGAAT
	-	TCTTACCTCTCCTGCGTATA
Vcp	+	CTTCAGGAGTTGGTTCAGTA
	-	AGGTCTTAGGATAGCAGGAT
Vdac1	+	CTCTGGTGCTTGGCTATG
	-	CCTGATACTTGGCTGCTATT
Gapdh	+	TGACCTCAACTACATGGTCTACA
	-	CTTCCCATTCTCGGCCTTG
mt-Co2	+	GTCCTCTATATCATCTCGCTAA
	-	GCATAGGTCTTCATAGTCAGT
mouse mtDNA	+	CCCATTCCACTTCTGATTACC
	-	ATGATAGTAGAGTTGAGTAGCG
mouse nucDNA	+	GTACCCACCTGTCGTCC
	-	GTCCACGAGACCAATGACTG
Aurkb	+	CTACGACCAGCAGAGGAT
	-	ACCATCAGTTCATAGCAGAG
Birc5	+	CATAAGGAGCACAGCCATA
	-	GGACAGAACAAGCCAGAG
Ccnb1	+	CAGCACTACCTATCCTACAG
	-	CTCAGAAGCAACAACATTCA
Cdc25c	+	TCCTCTGACTTCTCCTCTG
	-	GACTCTTCCTCCTCCATCT
Cdca2	+	TGTGCTTCGTTCTGTGTT

	-	GGTTCTCCTCCTTGTCATC
Cdca3	+	CCTGTGAGACCTGGATAGA
	-	GAGGCTTAGGCTTGAGTAG
Cenpe	+	CATTGCTTGGTGGTGGTA
	-	GTTGCTGCTGTGTCTCTT
Chtf18	+	TGGAAGACTACGAGGAAGA
	-	CAGGACAGGATTGCGATT
Ckap2	+	ACTTGTGCGACCTCCTAT
	-	GCTATAACTTCAGATGCTATGG
Sod1	+	GCTTCTCGTCTTGCTCTC
	-	GACAACACAACTGGTTCAC
Sod2	+	GTGTGCTGTATGAATGTGTT
	-	AGATGGTGAGACGAATGTG
Gpx1	+	GAGAAGTGCGAAGTGAATG
	-	CCTTAGGAGTTGCCAGAC
Ucp3		CTGCTCTTCTGCCTTCTC
		CATTCTGTCCTTCCACCAT
Catalase	+	TCAGGTGCGGACATTCTA
	-	ATTGCGTTCTTAGGCTTCT
Ant1	+	AACCAGACCGTAAGGAATAC
	-	TTCAGCATCAGTTCTTCAGT
U6	+	GCGCGTCGTGAAGCGTTC
	-	GTGCAG GGTCCGAGGT

Table S2. The RNA interference used in this study.

siRNA name	Sequence (5'-3')
ShcircSamd4/si-circSamd4-1	GCAAGCACGAGAATCATTA
ShcircSamd4/si-circSamd4-2	CAAGCACGAGGAATCATTA
Si-Nrf2	GCAGGAGAGGTAAGAATAA

Table S3. The results of mass spectrometry analysis after RNA pulldown related to Fig. 7A.

Table S4. The differentially expressed genes between Adv-circSamd4 and Adv-NC group.

Supplemental Video. 1-4 Time-lapse imaging of CMs after interventions corresponding to Fig. 3E. Video 1: PBS group; Video 2: H_2O_2 group; Video 3: H_2O_2+Adv-NC group; Video 4: H_2O_2+Adv-circSamd4 group. Time-lapse imaging started 12hr post-transduction (1/3 hr/Frame).